Jean BESTER, Ben GROENEWALD, Richardt WILKINSON

Cape Peninsula University of Technology

Electrical power system for a 3U CubeSat nanosatellite incorporating peak power tracking with dual redundant control

Abstract. *Since the advent of the CubeSat nanosatellite standard it has been embraced by many universities as an affordable means of conducting space science, with the backbone of any such mission being the supply of electrical power to the spacecraft's payloads. This paper details the design of a photovoltaic-battery based power supply utilising peak power trackers for solar array regulation and battery charging. Uniquely, the peak power tracking is executed by an active search algorithm, Perturb & Observe, in both analogue and digital form as a measure of redundancy.*

Streszczenie. *W artykule opisano projekt baterii fotowoltaicznych wykorzystujący układ śledzenia maksymalnej mocy do sterowania procesem wytwarzania energii i ładowania baterii. Wykorzystano algorytm Perturb & Observe. (**System fotowoltaicznego zasilania układów satelitarnych wykorzystujący układ śledzenia mocy maksymalnej**)*

Keywords: CubeSat, electrical power system, peak power tracking, perturb & observe.
Słowa kluczowe: zasilanie fotowoltaiczne, układ śledzenia mocy.

Introduction

Designing, building and ultimately launching a satellite in order to conduct space science and exploration has always been an expensive endeavour, something out of reach for most universities. This scenario has all but changed since the introduction of the CubeSat design specification in 1999 by aerospace engineering professor Jordi Puig-Sauri (from California Polytechnic State University) and professor Robert Twiggs (from the Department of Aeronautics & Astronautics at Stanford University) [1]. They recognised that in order to minimise design and, in particular, launch costs requires a low volume, lightweight nanosatellite, deployable from a standardised deployer (called a P-POD, Poly Picosatellite Orbital Deployer) which easily integrates with launch vehicles.

Therefore the standard CubeSat measures only 10x10x10cm and is called a 1U CubeSat, and is scalable up to 2U (20x10x10cm) and 3U (30x10x10cm) units. A 1U unit is restricted to 1.33kg and a 3U unit to 4kg. Since its inception many universities have taken up the concept with successful launches and operations having been conducted by California Polytechnic State University (CP-1, CP-3, CP-4), Aalborg University (AAU-CubeSat), Tokyo Institute of Technology (Cute-1.7 APD) and more recently École Polytechnique Federale de Lausanne (SwissCube), with future missions being planned by the Cape Peninsula University of Technology and Warsaw University of Technology. The goal of such university missions is to expose students to and familiarise them with the satellite engineering environment.

It is taken as given that these and any other satellites require electrical power to operate and fulfil their respective missions. Provision of electrical power to space vehicles is, perhaps, the most fundamental requirement of the satellite payload, with power system failure necessarily resulting in space mission failure [2].

The paper commences with an overview of satellite power systems, together with primary and secondary power sources. Top level design then discusses different power system topologies together with the design and test results of the peak power tracker.

Satellite electrical power systems

The electrical power system (EPS) of a satellite generates, stores, controls and distributes spacecraft electrical power, as is illustrated in Fig. 1. The payload demands for average and peak electrical power, together with the orbital profile, are important sizing factors affecting the solar array and battery unit, and must take into consideration power demands at beginning-of-life (BOL) and end-of-life (EOL) to enable the EPS to fulfil all of its top level functions. Top level functions are to supply a continuous source of electrical power to the satellite bus for the duration of the mission lifetime, control and distribute power to the satellite, provide power during periods of average and peak power demand, protect against bus faults and to monitor and communicate EPS health and status to the on-board computer (OBC).

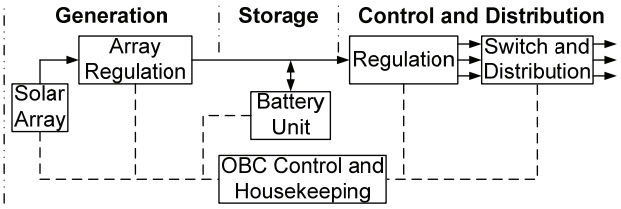

Fig.1. Breakdown of the electrical power system

This paper will focus on the regulation of the solar array power, together with detailing the solar array and battery unit as they greatly influence the choice of solar array regulator topology.

Primary power source – solar array

Given the size and weight constraints of a CubeSat, the only viable option for primary power is solar photovoltaics. Observing the current-voltage (I-V) characteristics of a solar cell in Fig. 2 a non-linear dependency between the voltage and current drawn can be noted. This creates a single point where the solar cell delivers its maximum power, called the maximum power point (MPP). It is thus important to note that the power available is dependent on the manner it is drawn from the cell.

Available solar cell technologies include silicon (Si), single junction (GaAs), dual junction ($GaInP_2$/GaAs) and triple junction ($GaInP_2$/GaAs/Ge). However, the only viable technology is triple junction. Compared to a Si-based cell it has much higher efficiency (of up to 27% compared to 17%) [3, 4], better radiation resistance [4] and better temperature coefficients [3], ensuring higher power delivery at EOL, given the same size array. They also have higher output voltages of 2.35V (against 0.6V for Si-cells), requiring fewer cells in series to attain usable voltage levels. A typical 3U CubeSat solar array configuration is two cells in series with three such groups in parallel, giving a power output of:

$$P_{OUT} = (n_s \cdot V_{MPP}) \cdot (n_p \cdot A \cdot J_{MPP})$$
$$= (2 \cdot 2.35)(3 \cdot 26.4 \cdot 16.3 \cdot 10^{-3}) \quad (1)$$
$$= 6.0675\text{W}$$

where n_s is the number of series cells, n_p is the number of parallel cells, V_{MPP} is the peak power point voltage, J_{MPP} is the peak power point current per cm^2 and A the solar cell area in cm^2.

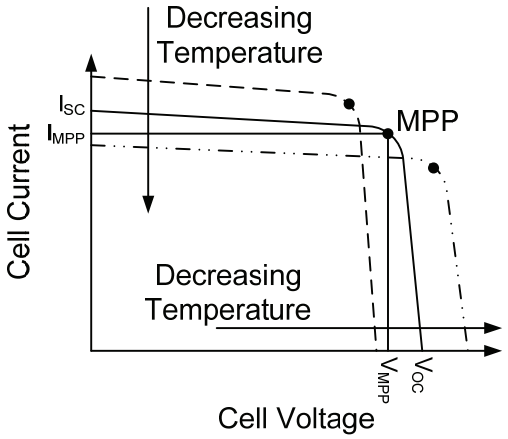

Fig.2. Solar cell characteristic I-V curve indicating the shifting MPP

Secondary power source - battery

Any spacecraft utilising photovoltaics as a primary power source requires a system to store energy for eclipse periods and peak-power demands, and batteries fulfil this role. Available battery technologies include nickel-metal hydride (NiMH), Lithium-ion (Li-ion) and Li-ion polymer (LiPo). The only battery technology viable for CubeSat use is that of Li-ion or LiPo, because of their high volumetric and gravimetric energy densities, resulting in a compact, flat battery design with a low magnetic signature; advantageous for the space restricted CubeSat [5]. They must though be operated under certain conditions.

An optimal discharge rate is C/3 or less (where C/x is the rated battery capacity divided by x) down to a depth of discharge (DOD) of 30% [5]. Operating the battery at rates such as C/1 and down to 80% DOD, for example, dramatically speeds up the decrease in capacity loss and increase in internal resistance (generally Li-ion based cells have efficiencies of up to 97% at BOL [6]). One technique to help the battery maintain its BOL capacity and high level of efficiency for as long as possible is by connecting two cells in series, doubling the battery bus voltage (V_{BUS}) and halving its discharge current. This can be done without the need for balancing circuitry [5].

A drawback of Li-ion based batteries is their high sensitivity to overcharge (resulting in overvoltage) [7] and this situation must be prevented by the charging circuitry.

Top level design choices (efficiency as a driver)

The design of an EPS for implementation on a CubeSat differs from the norm. Normally EPS design commences with a power budget to determine the size and capacity of the solar array and battery unit, respectively, required to adequately power the spacecraft. This approach is not feasible with CubeSats as the solar arrays are body mounted (unless provision is made for deployable wings) with the dimensions of the 3U (and thus the area available for affixing solar cells) being set by the CubeSat design specification [8].

The aim is to create the biggest solar array possible by covering the nanosatellite body with as many solar cells as possible, with the focus being how to best extract, distribute and store all energy available from the solar array in the most efficient manner. The choice of topology has an influence upon this, with the two options being either the traditionally more robust direct energy transfer (DET) type with dissipative shunt regulation or the more efficient non-DET with series regulation.

DET versus non-DET

With DET systems there is a direct connection between the solar array and battery unit (as load), with no active components in-between. All other systems are labelled as non-DET systems. DET systems are mostly of the shunt type and utilise shunt regulators, with non-DET systems being of the series type, employing maximum peak power trackers (MPPTs) as series regulators.

MPPTs work by placing a switch mode DC-DC converter between the solar array and the battery unit and maintaining the solar array's operating point at the MPP. It does this by dynamically changing the solar array's voltage operating point, allowing it to swing up to the MPP where it converts the input power to the equivalent output power, but at a different voltage and current [9, 10].

Shunt regulation works by having the solar array output voltage clamped to that of the fluctuating battery bus voltage. The bus then dictates the operating point on the solar array I-V curve (Fig. 2), with any excess current not required by the payloads being shunted into dissipative resistor banks.

A drawback of DET is that the solar array is only operated near its MPP when it is hot and the battery is fully charged [11]. This is because upon exiting eclipse the array is cold (with a high voltage, Fig. 2) and the battery is depleted (with a low voltage), creating a big difference between the V_{MPP} and V_{BUS}. As an example, consider a solar panel with three parallel groups of two series-connected triple-junction solar cells at -40°C connected to a 2000mAh Li-ion cell at 30% DOD. The battery clamps the solar array at 3.83V, causing it to deliver 1.323A and 5.069W. Operating at the MPP at this temperature would have delivered 7.112W, resulting in 28.73% loss in power. At a charge current of 1A (leaving 323mA to power payloads) it will take 36min to return the battery to full charge. Thus, only halfway through the sunlight period, when the solar array is hot, will the clamped array power (5.708W) be close to the MPP (6.151W), resulting in only 7.2% power loss. But, as has been shown in [12], the battery is already fully charged and the excess power will have to be shunted in order to prevent the battery from overcharging.

But also consider a MPPT with 90% efficiency. At -40°C it will extract 7.112·0.9=6.4W from the solar array and deliver 1.671A at 3.83V. Again leaving ±300mA for loads, the battery will recharge within 27min at 1.371A charge current. The 9min gained is not a lot, but if the satellite has power hungry payloads the extra 6.4–5.069=1.331W could be crucial.

Thus, the higher the MPPT efficiency, the stronger this argument becomes. Yet despite the efficiency loss, the majority of CubeSat missions still use the DET topology, either by using shunt regulation [13, 14, 15] or directly coupling the solar array to a voltage regulator without any MPPT control [16, 17], needlessly leaving precious energy unutilised in the solar array; energy which could have been used to minimise battery discharge during peak power demand periods, ensure a positive power margin at EOL and restore charge to the batteries quicker whilst maintaining normal satellite operations. Another short coming is the lack of redundancy, creating a scenario where even a partial failure in solar array regulator circuitry can

lead to a negative energy balance. The aim then is the development of a highly efficient MPPT with built-in redundancy.

Peak power tracking – Perturb & Observe

As shown in Fig. 2 the MPP of the solar array shifts as the solar array heats and cools, requiring a search algorithm to adjust the duty cycle of the MPPT DC-DC converter such that the solar array operating voltage is maintained at that of the MPP. One such algorithm is Perturb & Observe (P&O) [9]. It operates by making a change in the duty cycle and then multiplying the DC-DC converter output voltage and current to obtain the output power. The resulting value is then compared to the previous power value to ascertain whether the power increased or decreased because of the duty cycle perturbation. Should the output power have increased, the same duty cycle perturbation is repeated. Should it have decreased the perturbation direction is reversed. A new power measurement is made and compared to the previous one, and so the cycle repeats in a never ending loop.

A disadvantage of the algorithm is its ability to potentially track in the wrong direction under rapid atmospheric changes as it cannot discriminate whether changes in the MPPT output power were caused by variations in the atmosphere or purposeful duty cycle changes [18]. This can be guarded against by setting lower and upper duty cycle limits, at which point the perturbation direction must be changed. A great advantage of the P&O algorithm is its simplicity, easily implementable with either analogue or digital circuitry, as will be exploited by this EPS design.

The peak power tracker

As shown in Fig. 3 & 4 the MPPT consists of a boost DC-DC converter and associated control circuitry, with the solar panel as input and the battery unit as output. The control circuitry executes the P&O algorithm, in both analogue (Fig. 3) and digital (Fig. 4) form. A microcontroller (MCU) can more efficiently track the MPP and implement improved versions of the algorithm whilst being easily tuneable, but it is more susceptible to failure due to radiation damage. The analogue implementation then forms a back-up as its discrete circuitry is more robust than an MCU and, although it is not as efficient at tracking the MPP as the MCU, the satellite will still be able to operate in case of MCU failure.

In both Fig. 3 & 4 it can also be seen that only the output current and not the output voltage is being measured. As the output voltage is clamped to the slow changing battery voltage, it can be considered as constant between samples. Thus, the output current alone indicates an increase or decrease in power and only this need to be measured [19]. Also, as the DC-DC converter's output is slaved to the battery voltage a change in duty cycle varies the DC-DC converter input voltage and in this manner the output power of the solar array can be controlled [11].

A simple yet novel control method is used to facilitate charging of the battery unit whilst doubling as overvoltage protection. Whilst the battery unit is below 8.4V and still charging, the MPP will be tracked. Any current not utilised by the payloads will charge the battery unit. Once the battery unit reaches the full charge voltage of 8.4V, MPP tracking is halted to prevent overcharge. Hysteresis is incorporated such that once the battery unit voltage decreases to 8V the MPPT is restarted and charging resumed.

Analogue P&O control

Fig. 3 shows the analogue circuitry used to execute the P&O algorithm using the clocked auto-oscillation method [19, 20]. The output current of the boost DC-DC converter is measured using a current shunt monitor, the output of which is sent to the differentiator. The task of the differentiator is to indicate whether the slope of the current shunt output is negative or positive, with other words, whether the output current (and thus the power) is decreasing or increasing. The op-amp around which the differentiator is based has its non-inverting input tied to ½ V_{CC}, causing its output to be at ½V_{CC} during quiescent states or when the change in current is zero. If the DC-DC converter output current decreases, the differentiator's output voltage rises above ½V_{CC}, and vice versa.

The comparator then uses the output voltage of the differentiator to indicate by logic level whether the DC-DC converter output current is increasing or decreasing. The comparator's non-inverting input is connected to the differentiator output whilst its inverting input is biased slightly above ½V_{CC}. This biasing is to prevent the comparator from triggering erratically during quiescent states due to noise which causes the differentiator output to perturb around ½V_{CC}. When the MPPT output current increases the decrease in differentiator output forces the comparator output to go or stay LOW. A decrease in output current causes the differentiator output to rise and when it increases past the comparator bias voltage the comparator output is HIGH. Thus, a comparator HIGH output indicates decreasing output power, and a LOW output increasing output power.

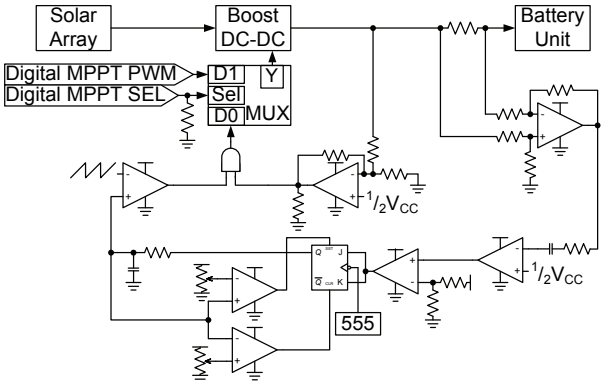

Fig.3. The analogue circuitry executing the P&O algorithm

The comparator output is connected to a T (Toggle) flip-flop. When the comparator output is HIGH the flip-flop output toggles its state on each negative going clock edge. With the comparator output LOW the flip-flop output state is latched. The flip-flop output is integrated by the RC network at its output, and thereby becomes the V_{REF} for the PWM. V_{REF} is a triangle wave riding upon a DC offset, creating the duty cycle perturbation needed to measure $\Delta I_{OUT}/\Delta D$.

Overall analogue P&O operation

Suppose the system starts with V_{REF} below the maximum power point, with the flip-flop output HIGH. The duty cycle and the output current will both be ramping up, forcing the comparator output LOW and latching the flip-flop output. When the MPP is overshot, the output current decreases. This is sensed and the comparator output goes HIGH, prompting the output of the flip-flop to toggle LOW on the next clock cycle and the ramp on V_{REF} changes direction. The output current starts to increase again, and the process repeats, yielding a small oscillation around the MPP.

To summarise, if the output current (and thus the output power) is increasing the flip-flop output state is correct and must be latched. If the current is decreasing the flip-flop output is incorrect and must be toggled.

Digital P&O control

The digital MPPT control implementation is shown in Fig. 4, with the P&O algorithm executed as a logic sub-routine on an MCU. The digital implementation is much simpler than its analogue counterpart as the P&O algorithm is easily translatable into flowchart form (Fig. 5) and thus not difficult to port to C-code.

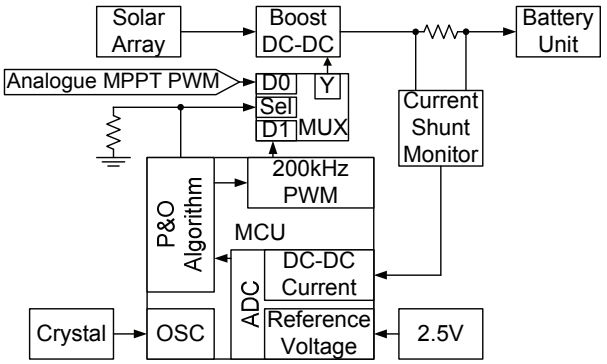

Fig.4. The digital circuitry executing the P&O algorithm

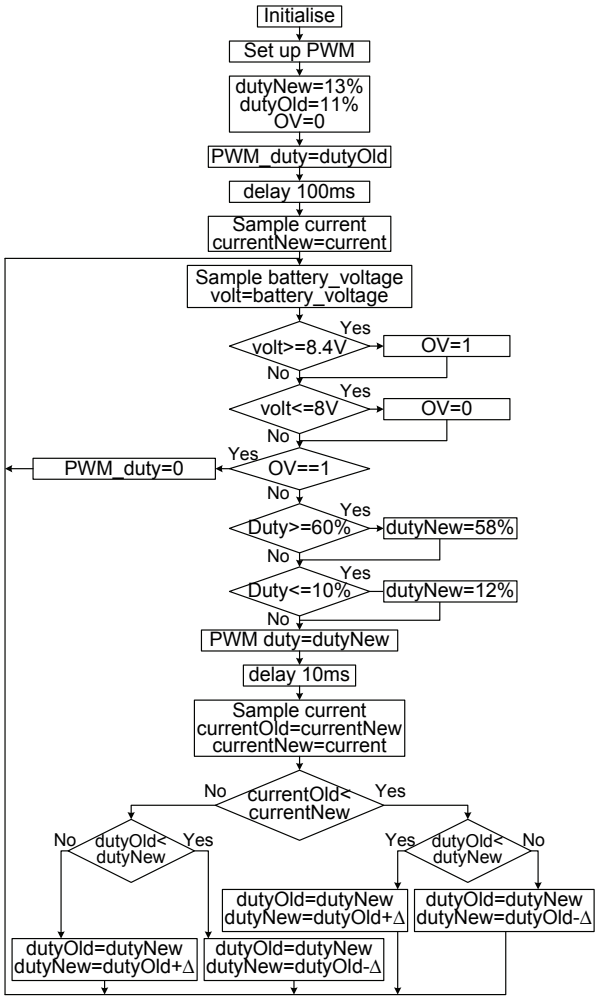

Fig.5. The digital MPPT flowchart

As mentioned, the main concept is to have the digital version operate as the main MPPT control, with the analogue version as back-up. The switch over between the digital and analogue control of the MPPT is then handled by a multiplexer (MUX) (as in Fig. 3 & 4) to route the designated PWM signal to the MOSFET driver of the DC-DC converter. The control line of the MUX is passively pulled LOW, switching by default to the analogue control when the EPS powers up. To ensure than the MCU has started up correctly and is able to take over control of the MPPT it must pull the MUX control line HIGH.

Test results

A test solar array was constructed to evaluate the MPPT by connecting ten Si-based solar cells in series to achieve a V_{MPP} as close as possible to 4.7V, with incandescent light bulbs powered from a DC power supply providing adjustable levels of illumination. To ensure that the MPPT maintains its efficiency levels under any condition of solar array illumination it was tested under levels of low (P_{MPP}=1.95W), medium (P_{MPP}=3.5W) and full (P_{MPP}=5.65W) insolation. To simulate rapid changes in insolation and to measure the MPPT's tracking response the insolation was stepped from low to full and back.

Table 1 shows the test results for the digital MPPT, with excellent efficiency levels of 93.41% under full insolation being achieved and maintained at 94.28% under low insolation. Most tracking losses can be attributed to the inherent perturbation around the MPP and can be improved by making the step size smaller. It must also be mentioned that the efficiency values include the power consumption of the control circuitry, creating an ideal opportunity for even higher efficiency levels if lower power circuitry can be implemented, such as an improved MCU.

Table 1. Digital MPPT efficiency results

Low Insolation		
P_{MPP}=1.9451W	P_{OUT}=1.9389W	η=94.28%
Medium Insolation		
P_{MPP}=3.5054W	P_{OUT}=3.2979W	η=94.08%
Full Insolation		
P_{MPP}=5.6533W	P_{OUT}=5.5876W	η=93.41%

The step response of the digital MPPT (Fig. 6) showed it to remain stable, exhibiting no oscillations, and no erratic tracking behaviour being observed under rapid insolation changes during testing. At worst, the algorithm takes 419ms to settle at the new MPP which compares well to the 1s settling time obtained by [21].

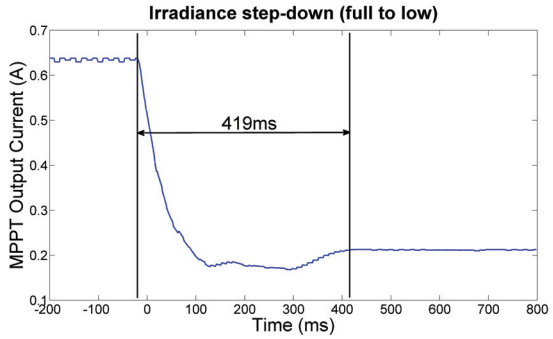

Fig.6. The worst case step response of the digital MPPT occurs when the irradiance steps from high to low

Table 2 shows the results of the analogue MPPT, with satisfactory efficiency levels of 90.21% under low insolation and maintained at 91.26% at full insolation. This is on average 4% less than the digital MPPT, qualifying it as a robust back-up solution. The step response of the analogue MPPT (Fig. 7) showed it to remain stable with no oscillation and no erratic tracking behaviour being detected. At worst the algorithm takes 329ms to settle at the new MPP, which compares well with the 300ms obtained by [19].

From Fig. 7 it is also clear why the analogue MPPT is less efficient than its digital counterpart. The MPPT output current (and thus the output power) consistently overshoots the MPP by a large margin as the algorithm perturbs around the MPP. To minimise this overshoot the clock frequency has been increased and the V_{REF} rate of change slowed down to the point where a balance was struck between accurate tracking at low irradiance levels and power loss due to overshoot at high irradiance levels.

Table 2. Analogue MPPT efficiency results

Low Insolation		
P_{MPP}=1.9451W	P_{OUT}=1.7547W	η=90.21%
Medium Insolation		
P_{MPP}=3.5054W	P_{OUT}=3.2795W	η=93.56%
Full Insolation		
P_{MPP}=5.6533W	P_{OUT}=5.1537W	η=91.16%

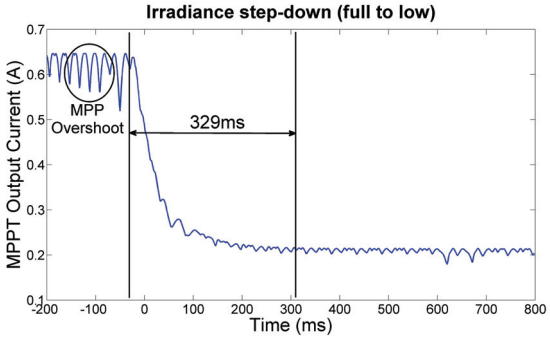

Fig.7. The worst case step response of the analogue MPPT occurs when the irradiance steps from high to low

Conclusions

The experiments have shown how non-DET has a clear efficiency advantage over DET by employing MPPTs which actively track and operate the solar array at its MPP, even as it shifts. This advantage is then further built upon by implementing the P&O peak power tracking algorithm in both digital (main control) and analogue (back-up) form, creating an efficient EPS with built-in redundancy.

The digital version is based around an MCU, and achieved excellent efficiency results of 94%. The analogue version, based on the clocked auto-oscillation method, achieved 90% efficiency, qualifying it as a robust back-up. In the final implementation multiple MPPTs will be paralleled, with each solar panel having its own MPP tracked, further enhancing the overall efficiency of the EPS [22].

REFERENCES

[1] A. Toorian, K. Diaz, and S. Lee, "The cubesat approach to space access," in *Proceedings of the 2008 IEEE Aerospace Conference*. New York, NY: IEEE, 2008, pp. 1-14.

[2] J. Stark, *Spacecraft Systems Engineering*, 3rd ed. West Sussex: Wiley, 2003, ch. Electrical power systems, pp. 325-354.

[3] N. Fatemi, H. Pollard, H. Hou, and P. Sharps, "Solar array trades between very high-efficiency multi-junction and Si space solar cells," in *Conference Record of the 28th IEEE Photovoltaic Specialists Conference (PVSC 2000)*. New York, NY: IEEE, 2000, pp. 1083-1086.

[4] M. R. Reddy, "Space solar cells - tradeof analysis," *Solar Energy Materials and Solar Cells*, vol. 77, no. 2, pp. 175-208, May 2003.

[5] V. McLaren, C. Clark, E. Simon, and B. Hendel, "Lithium ion polymer cell for small satellites," in *Proceedings of the 2008 NASA Aerospace Battery Workshop*. NASA, 2008, published on CD-ROM.

[6] J. Reynaud, C. Alonso, P. Aloisi, C. Cabal, B. Estibals, G. Rigobert, G. Sarre, H. Rouault, D. Mourzagh, F. Mattera, and S. Genies, "Multifunctional module lithium-ion storage and photovoltaic conversion of solar energy," in *Conference Record of the 33rd IEEE Photovoltaic Specialists Conference (PVSC '08)*. New York, NY: IEEE, 2008, pp. 1-5.

[7] Microchip, *Application note AN947: power management in portable applications: charging lithium-ion/lithium-polymer batteries*, 2004.

[8] Anon., *CubeSat design specification*, 12th ed. San Luis Obispo, CA: California Polytechnic State University, 2009.

[9] D. Hohm and M. Ropp, "Comparative study of maximum power point tracking algorithms," *Progress in Photovoltaics: Research and Applications*, vol. 11, no. 1, pp. 47-62, November 2002.

[10] J. McDermott, *Space Mission Analysis and Design*, 3rd ed. New York, NY: Springer, 2007, ch. Power, pp. 407-427.

[11] D. Snyman and J. Enslin, "Simplified maximum power point controller for pv installations," in *Conference Record of the 23rd IEEE Photovoltaic Specialists Conference (PVSC '93)*. New York, NY: IEEE, 1993, pp. 1240-1245.

[12] C. Clark and A. Lopez, "Power system challenges for small satellite missions," in *Proceedings of the 2006 Small Satellites, Systems and Services Symposium*, D. Danesy, Ed. The Netherlands: ESA, 2006, published on CD-ROM.

[13] F. Jordan, "Electrical power system (eps): phase b," Master's thesis, Haute École d'Ingénierie et de Gestion du Canton de Vaud, Yverdon, 2006.

[14] P. Thirion, "Design and implementation of on-board electrical power supply of student nanosatellite oufti-1 of university of Liège," Master's thesis, University of Liège, Liège, 2009.

[15] J. Schaffner and J. Puig-Suari, "The electronic system design, analysis, integration, and construction of the Cal Poly State University CP1 cubesat," in *Proceedings of the 16th Annual AIAA/USU Conference on Small Satellites*. Logan, UT: Utah State University Research Foundation, 2002, published on CD-ROM.

[16] M. Long, A. Lorenz, G. Rodgers, E. Tapio, G. Tran, K. Jackson, R. Twiggs, and T. Bleier, "A cubesat derived design for a unique academic research mission in earthquake signature detection," in *Proceedings of the 16th Annual AIAA/USU Conference on Small Satellites*. Logan, UT: Utah State University Research Foundation, 2002, published on CD-ROM.

[17] R. Chan, R. Benerjee, and A. Jani, "Win-cube project: electrical power system phase two critical design review," Bachelor's thesis, University of Manitoba, Winnipeg, 2008.

[18] I. Kim and M. Youn, "Single-loop maximum power point tracker with fast settling time," in *Proceedings of the 30th Annual Conference of IEEE Industrial Electronics Society (IECON '04)*. New York, NY: IEEE, 2004, pp. 862-866.

[19] K. Lee, J. Niu, and G. Lin, "A simplified analog control circuit of a maximum power point tracker," in *Conference Record of the 33rd IEEE Photovoltaic Specialists Conference (PVSC '08)*. New York, NY: IEEE, 2008, pp. 1-3.

[20] C. Sullivan and M. Powers, "A high-efficiency maximum power point tracker for photovoltaic arrays in a solar-powered race vehicle," in *Conference Record of the 24th Annual IEEE Power Electronics Specialists Conference (PESC '93)*. New York, NY: IEEE, 1993, pp. 574-580.

[21] J. Lee, H. Bae, and B. Cho, "Advanced incremental conductance MPPT algorithm with a variable step size," in *Proceedings of the 12th International Power Electronics and Motion Control Conference (EPE-PEMC '06)*. New York, NY: IEEE, 2006, pp. 603-607.

[22] S. Poshtkouhi, J. Varley, R. Popuri, and O. Trescases, "Analysis of distributed peak power tracking in photovoltaic systems," in *Proceedings of the 36th Annual Conference of IEEE Industrial Electronics Society (IECON '10)*. New York, NY: IEEE, 2010, pp. 942-947.

***Authors**: BTech Jean Bester, MSc Ben Groenewald, PhD Richardt Wilkinson, French South African Institute of Technology, Department of Electrical Engineering, Centre for Instrumentation Research, Cape Peninsula University of Technology, Symphony Way, Bellville, Cape Town, 7530, South Africa, email: bester.jean@gmail.com, groenewaldb@cput.ac.za, wilkinsonr@cput.ac.za.*